1992

A Real Gas Simulation of a Refrigeration Compressor and its Performance Comparison for CFCs and Non-CFCs

K. T. Ooi
Nanyang Technological University

T. N. Wong
Nanyang Technological University

E. C. Kwek
Matsushita Refrigeration Industries; The Republic of Singapore

A REAL GAS SIMULATION OF A REFRIGERATION COMPRESSOR AND ITS PERFORMANCE COMPARISON FOR CFCS AND NON-CFCS

K.T., OOI and T.N., WONG
Nanyang Technological University, Singapore 2263

E.C., KWEK
Matsushita Refrigeration Industries (S) Pte Ltd
1 Bedok South Road, Singapore 1646

ABSTRACT

CFCs have been very widely used in many household appliances and industries. They are chemically stable, non-toxic, non-flammable and are friendly to most other materials except the environment. They cause depletion of the ozone layer and global warming. Urgent need is required to replace this substance globally. It is expected that any production of fully halogenated hydrocarbons (CFCs) is expected to be phased out completely by the end of this century. Among the most acceptable alternatives of the existing CFCs for R12 and R11 are HFC134a and HCFC123 respectively.

For a given refrigeration system, replacing a new refrigerant may mean the alteration of the whole or part of the system design in order to maintain the system performance. And the amount of alterations depend on the degree of similarities of the properties of the new refrigerant to that of the old one. A computer simulation of the system plays an important part in the decision making stage before actual design alterations take place. It gives an insight into the expected performance and possible changes that may be done. This paper presents predicted results of a small rolling piston refrigeration compressor using physical geometries and dimensions of the compressor which was designed for R12, when using R134a, R22 and R502 as the refrigerant. Comparison of pressure-volume histories and compressor performance parameters for R12, R22, R502, and R134a are presented. Similarities and differences in the performance are shown and discussed. The properties of the refrigerant were simulated using a real gas equation of state. Accounts on the simulation model itself are also given.

1. NOMENCLATURE

A	area, m^2
a	radius ratio, R_r/R_c
C_d	coefficient of discharge
e	eccentricity
F_x	pressure differential force across vane in x direction, N
F_y	pressure differential force across vane in y direction, N
F_s	vane spring force, N
F_a	inertia force of vane, N
F_{vt}	tangential force at vane tip, N
F_{vn}	normal force at vane tip, N
F_{t1}, F_{t2}	tangential forces at vane side contact points, N
F_{n1}, F_{n2}	normal forces at vane side contact points, N
h	blade height, m or specific enthalpy J/kg
I_r	moment of inertia of roller, kgm^2
k	vane spring constant N/m
l	cylinder length, m
L_v	friction loss at vane tip, W
L_s	friction loss at vane side, W
L_{ec}	friction loss between eccentric and cylinder head face, W
L_{rc}	friction loss between roller and cylinder head face, W
L_{re}	friction loss between the roller and eccentric, W
m	mass of fluid, kg
M_{ec}	friction moment from eccentric to cylinder head face, Nm
M_{er}	friction moment from eccentric to roller, Nm
M_{rc}	friction moment from roller to cylinder head face, Nm
M_v	mass of vane, kg
P_b, P_c	pressure in suction and compression chambers, N/m^2

P	pressure, N/m^2
P_R	pressure ratio, P/P_c
P_s, P_d	suction and discharge pressures, N/m^2
Q	heat transfer, J
R	gas constant, $J/(kgK)$
R_c	cylinder radius, m
R_r	roller outer radius, m
R_e	radius of eccentric, m
R_s	shaft radius, m
R_v	vane tip radius, m
T	temperature, K
T_R	temperature ratio, T/T_c
t_b	blade thickness, m
u	specific internal energy, J/kg
V_s	specific volume, m^3/kg
V_c, V	Volume, m^3
$\overline{V}$	velocity, m/s
V_t	sliding velocity at vane tip, m/s
x	vane extension, m
$x_{(max)}$	maximum spring compression, m
w	work, J
Z_c	critical compressibility, $P_c/(R\rho_c T_c)$
θ	angular position of rotor, radian
α	offset angle of rolling piston centre, °
δ	radial clearance between roller and cylinder at $\theta = 0$, m
δ_1	clearance between roller and cylinder head face, m
δ_2	radial clearance between roller and eccentric, m
δ_e	vane protrusion, N
δ_3	clearance between eccentric and cylinder head face, m
η	viscosity of lubricating oil, Ns/m^2
ω	angular velocity of eccentric, rad/s
ω_r	angular velocity of rolling piston, rad/s
μ_s	coefficient of friction at vane side
μ_v	coefficient of friction at vane tip
ρ_R	density ratio, ρ/ρ_c
	time differential

2. INTRODUCTION

Since the Molina and Rowland first hypothesized the ozone destruction by CFCs, the usage of CFCs (e.g. R12 and R11) which have high ozone depletion potential (ODP) will be phased out. Alternatives to the CFCs are suggested.

In refrigerator applications, R12 is commonly used. Amongst its potential alternatives are R22, R502 and R134a. Conventionally R22 and R502 were not used in refrigerator due to their high condensing pressures. Although the use of HCFCs were not be restricted but the substitute of R22 and R502 to that of the R12 is a temporary one. This is because their ODP and green house effects still remains, although much lesser than R12 and their usage is subjected to possible phase out by the year 2040 (10). The R134a has long been regarded as a substitute to the R12. It has zero ODP and zero green house effects. But the current trend of the substitute of R134a to R12 is restricted by the availability of the compatible material, mainly lubricating oil in the refrigeration industries.

In a vapour-compression refrigeration system, there are generally four basic components i.e. a compressor, a condenser, an expansion valve and an evaporator. The compressor is the only work absorbing component in the cycle. The matching of the right components to achieve an effective cycle is important. This paper presents preliminary investigations over the predicted performance of the compressor which was designed for R12 using CFC alternatives. Predicted results on variation of pressure-angle history, pressure-volume diagram, temperature variation will be presented. Variation in the indicated work done will also be discussed.

3. MATHEMATICAL MODELLING

3.1 Introduction

Rolling piston compressors are commonly found in air compression and refrigeration industries. They are geometrically simple machines with one roller (or rolling piston), a cylinder, a spring and a vane. They are highly reliable. Fig. 1 shows a schematic configuration of the compressor. During the operation the piston rolls along the inner wall of the cylinder. Within the roller and the cylinder wall there exists two chambers which are separated by the vane and the roller-cylinder contact. While one chamber undergoes compression/delivery process the other undergoes suction. The process is cyclic and it takes two revolutions to complete a cycle. The existence of the compression spring is to ensure that the vane tip-roller contact is maintained throughout the operational process. The overall performance of a given machine depends on the balance of compression, frictional effects, leakage effects, suction and discharge effects.

With the availability of high speed computers, a complete modelling of the machine that caters for geometrical, fluid flow, heat transfer, dynamic and stress effects may be done with comparative ease. This section briefs the simulation of the machine. It accounts for geometric, thermodynamic and frictional effects. Where a real gas equation was used to describe the state of the refrigerating medium.

A basic model considering perfect seal, adiabatic will be presented. The basic model consists of geometric, thermodynamics and dynamics formulations. The model allows the variation of refrigerating fluid pressure, temperature and mass flow to be evaluated in relation to the geometrical configuration and the operating conditions of the machine. The indicated power may be obtained from the integration of the predicted pressure volume diagram.

3.2 Geometry Model

The geometry model of the compressor accounts for all important parameters which are within the working chamber of the compressor which may affect the performance of the compressor.

Refer back to Fig.1 the chamber volume trapped within the roller, cylinder and the vane may be given by,

$$V(\theta)=\frac{hR_c^2}{2}\left((1-a^2)\theta-\frac{(1-a)^2}{2}\sin 2\theta-a^2\sin^{-1}\left(\left(\frac{1}{a}-1\right)\sin\theta\right)-a(1-a)\sin\theta\sqrt{1-\left(\frac{1}{a}-1\right)^2\sin^2\theta}\right) \quad \ldots(2.1)$$

To account for the vane thickness, the volume given by eqn. (2.1) must be subtracted away the volume occupied by the vane extension:

$$V'(\theta)=V(\theta)-\frac{th\delta_\epsilon}{2} \quad \ldots(2.2)$$

Where

$$\delta_\epsilon=R_c(1-(1-a)\cos\theta-\sqrt{(1-a)^2\cos^2\theta+2a-1}) \quad \ldots(2.3)$$

3.3 Valve Flow Model

The suction port is assumed as a simple orifice without a valve. The effective flow area may be accounted for by introducing a discharge coefficient on the calculated geometrical area. The flow through the suction port is assumed to be one dimensional adiabatic flow. The isentropic efficiency is accounted for by lumping it into the discharge coefficient. Reversed flows are taken into consideration where the lumped discharge coefficient is assumed constant through out the suction process. The same value of the discharge coefficient is also used for reversed flows.

The discharge port is covered with a reed valve. The flow area can be the valve port area or the valve lift annulus area. The latter must be determined from the instantaneous valve deflection. The effective flow area is taken as the area which imposes more restrictions to the flow. Assumptions as in suction flow are applicable.

By first assuming the flow through the valve is isentropic, the flow velocity may be calculated.

$$\overline{V} = \sqrt{2(h_1 - h_2^{is})} \qquad \ldots(3.1)$$

Where suffixes 1 and 2 denote the conditions of the fluid upstream and downstream of the valve port respectively. The mass flowrate can be found by,

$$\frac{dm}{d\theta} = \frac{C_d A \overline{V}}{v_{s2}} \omega \qquad \ldots(3.2)$$

Where h_2^{is} is the downstream enthalpy assuming an isentropic expansion. To obtain the enthalpy the knowledge of the downstream specific volume and the temperature must be known. These information may be obtained by solving the equation of state as shown in eqn. (4.9) using Newton Raphson iterative method.

Where C_d is the discharge coefficient which accounts for the effective flow area and the isentropic efficiency, for actual non-isentropic flow. The choke flow condition is taken into the consideration by taking the maximum flow velocity to be equal to the sonic velocity at the throat of the port.

4. THERMODYNAMICS MODEL

In the thermodynamics model (3) the relationships within pressure, temperature and the mass will be formulated. These three unknowns were related using the energy conservation relation, mass conservation relation and the equation of state of a real gas. Brief account of the model are given below.

4.1 Pressure, Temperature And Mass Relationships

To obtain the relationship of the state of the working medium of the compressor, applying the First Law of Thermodynamics to the control volume by taking the boundary of the chamber as the boundary of the control volume and neglecting the kinetic and potential energy:

$$\frac{dQ_c}{d\theta} + \sum \frac{dm_i}{d\theta} h_i = \frac{dw_i}{d\theta} + \sum \frac{dm_o}{d\theta} h_o + \frac{d}{d\theta}(m u_c) \qquad \ldots(4.1)$$

where subscripts i and o denote inlet and outlet.

Taking the work term as the mechanical work:

$$dw = P dV_c \qquad \ldots(4.2)$$

Form the relationship of the enthalpy:

$$h = u + P v_s \qquad \ldots(4.3)$$

The pressure is a function of the temperature and the specific volume:

$$P = P(T, V_s) \qquad \ldots(4.4)$$

where the specific volume is given by:

$$V_s = V_c / m_c \qquad \ldots(4.5)$$

After the manipulation, the following expressions may be obtained,

$$\frac{dP_c}{d\theta} = \frac{\frac{1}{V_s}\left(\left(\frac{\partial P}{\partial v_s}\right)_T \frac{(\partial h/\partial T)_{v_s}}{(\partial P_c/\partial T_c)_{v_s}} \frac{dv_s}{d\theta} + \left(\frac{\partial h}{\partial V_c}\right)_T \left(\frac{\partial V_c}{\partial \theta}\right)\right) - \frac{1}{V_c}\left(\sum \frac{dm_i}{dm_\theta}(h_i - h_c) - \sum \frac{dm_o}{d\theta}(h_o - h_c)\right)}{1 - \frac{1}{V_s}\frac{(\partial h/\partial T)_{v_s}}{(\partial P_c/\partial T_c)_{v_s}}} \qquad \ldots(4.6)$$

and

$$\frac{dT_c}{d\theta} = \left(\frac{dP_c}{d\theta} - \left(\frac{\partial p}{\partial V_s}\right)_T \frac{dV_c}{d\theta}\right) \frac{1}{\left(\frac{\partial P_c}{\partial T_c}\right)_v} \qquad \ldots(4.7)$$

The mass in the working chamber can be obtained from the continuity equation, i.e.

$$\frac{dm_c}{d\theta} = \frac{dm_i}{d\theta} - \frac{dm_o}{dm_\theta} \qquad \ldots(4.8)$$

Where the two main sources of the m_i and the m_o are from suction and discharge flows through the respective ports.

The partial derivatives for refrigerant properties appeared in the above equations can be obtained by differentiating eqns. (4.9) to (4.14) below.

4.2 Simulation Of Refrigerant Properties

Refrigerant properties used in the analysis are simulated using real gas equations. The Martin-Downing type of equations (8) for refrigerant vapour are used for R12, R22 and R502. Where the equation of state is given in the form,

$$P = \frac{RT}{(V_s - \beta)} + \sum_{i=2}^{i=5} \frac{A_i + B_i T + C_i e^{-KT/T_c}}{(V_s - \beta)^i} \qquad \ldots(4.9)$$

The enthalpy is given as,

$$H = aT + \frac{bT^2}{2} + \frac{cT^3}{3} + \frac{dT^4}{4} - \frac{f}{T} + JPV + J\sum_{i=2}^{i=5} \frac{A_i}{(i-1)(V_s - b)^{i-1}} + Je^{-KT/T_c}\left(1 + \frac{KT}{T_c}\right)\sum_{i=2}^{i=5} \frac{C_i}{(i-1)(V_s - b)^{i-1}}$$

..(4.10)

The entropy is given as,

$$S = a(ln10)logT + bT + \frac{cT^2}{2} + \frac{dT^3}{3} - \frac{f}{2T^2} + JR(ln10)\log(V_s - b) - J\sum_{i=2}^{i=5} \frac{B_i}{(i-1)(V_s - b)^{i-1}} \qquad ..(4.11)$$

For the properties of R134a (which is not available in (8)), the Piao et. al type of equations (9) are used. These equations cater for wider range of applicability. It covers up to compressed liquid state properties. The equation of state is given in the form,

$$P = P_c\left(\frac{T_R \rho_R}{Z_c} + \sum_{i=2}^{i=9}\left(a_{i1} + \frac{a_{i2}}{T_R} + \frac{a_{i3}}{T_R^2} + \frac{a_{i4}}{T_R^3} + \frac{a_{i5}}{T_R^5}\right)\rho_R^i\right) \qquad \ldots(4.12)$$

The enthalpy is given as,

$$H = T_c R Z_c (f_R + T_R\left(\sum_{i=2}^{i=9}\left(\frac{a_{i2}}{T_R^2} + 2\frac{a_{i3}}{T_R^3} + 3\frac{a_{i4}}{T_R^4} + 5\frac{a_{i5}}{T_R^6}\right)\frac{\rho_R^{i-1}}{i-1} - \frac{1}{Z_c}\ln\rho_R\right) + \sum_{i=2}^{i=9}\left(a_{i1} + \frac{a_{i2}}{T_R} + \frac{a_{i3}}{T_R^2} + 2\frac{a_{i4}}{T_R^3} + 3\frac{a_{i5}}{T_R^5}\right)\rho_R^{i-1}$$

$$+ \frac{T_R}{Z_c} + \frac{T_R}{Z_c}\left((c_1 - 1)\ln\frac{T_R}{T_R^0} + c_2(T_R - T_R^0) + c_3\frac{\left(T_R^2 - (T_R^0)^2\right)}{2} + c_4\frac{\left(T_R^3 - (T_R^0)^3\right)}{3} + c_s\right) \qquad \ldots(4.13)$$

where,

$$f_R = \sum_{i=2}^{i=9}\left(a_{i1} + \frac{a_{i2}}{T_R} + \frac{a_{i3}}{T_R^2} + \frac{a_{i4}}{T_R^3} + \frac{a_{i5}}{T_R^5}\right)\frac{\rho_R^{i-1}}{(i-1)} + \frac{T_R}{Z_c}\ln\rho_R + \frac{1}{Z_c}\{(c_1 - 1)\left(T_R - T_R^0 - T_R\ln\frac{T_R}{T_R^0}\right) - c_2\frac{(T_R - T_R^0)^2}{2}$$

$$- c_3\frac{\left(T_R^3 - 3(T_R^0)^2 T_R + 2(T_R^0)^3\right)}{6} - c_4\frac{\left(T_R^4 - 4(T_R^0)^3 T_R + 3(T_R^0)^4\right)}{12} - (T_R - T_R^0)c_s - c_f\} \qquad \ldots(4.13a)$$

The entropy is given as,

$$S = RZ_c\left(\sum_{i=2}^{i=9}\left(\frac{a_{i2}}{T_R^2} + 2\frac{a_{i3}}{T_R^3} + 3\frac{a_{i4}}{T_R^4} + 5\frac{a_{i5}}{T_R^6}\right)\frac{\rho_R^{i-1}}{i-1} - \frac{1}{Z_c}\ln\rho_R -\right.$$

$$\left.\frac{1}{Z_c}\left((c_1 - 1)\ln\frac{T_R^0}{T_R} - c_2(T_R - T_R^0) - c_3\frac{\left(T_R^2 - (T_R^0)^2\right)}{2} - c_4\frac{\left(T_R^3 - (T_R^0)^3\right)}{3} + c_s\right)\right) \qquad \ldots(4.14)$$

Where a_{21} to a_{95}, c_1 to c_4, c_s and c_f are coefficient values depending on freon properties.

4.3 Frictional Analysis

To determine the friction losses of the compressor, the vane and the roller dynamics must be considered. The information about the vane sliding velocity, roller velocity must be obtained. There are six areas where the friction loss may take place (2,4,5,6).

These are friction losses occurred at the following regions (see Fig. 2 and Fig. 3):-

i. Eccentric and the inner surface of the roller,

$$L_{re} = (\omega - \omega_r) M_{er} \quad \ldots(4.15)$$

ii. Roller face and the cylinder head face,

$$L_{rc} = M_{rc}\omega_r \quad \ldots(4.16)$$

iii. Eccentric face and the cylinder head face,

$$L_{ec} = M_{ec}\omega \quad \ldots(4.17)$$

iv. Vane tip and roller,

$$L_v = V_t F_{vt} \quad \ldots(4.18)$$

Where,

$$V_t = R_r\omega_r + e\,\omega\cos\theta/\cos\alpha \quad \ldots(4.19)$$

v. Vane sides and vane slot,

$$L_s = (F_{t1} + F_{t2})\dot{x} \quad \ldots(4.20)$$

vi. Outer roller surface and the inner cylinder surface

The item (vi) can be ignored if it assumes that there exists no contact forces between outer roller surface and the cylinder. In the above eqns. other terms are defined as follow:

$$M_{rc} = 2\pi\omega_r\eta(R_r^4 - R_e^4)/\delta_1 \quad \ldots(4.21)$$

$$M_{ec} = \pi\eta\omega(2R_e^4 - R_s^4)/\delta_3 \quad \ldots(4.22)$$

$$M_{er} = 2\pi\eta(\omega - \omega_r)lR_e^2/\delta_2 \quad \ldots(4.23)$$

$$F_x = (P_c - P_b)x\,l \quad \ldots(4.24)$$

$$F_s = k(x_{(max)} - x) \quad \ldots(4.25)$$

$$F_a = -M_v\ddot{x} \quad \ldots(4.26)$$

$$F_y = \left(P_d b - P_c\left(\frac{t_b}{2} + R_v\sin\alpha\right) - P_b\left(\frac{t_b}{2} - R_v\sin\alpha\right)\right)l \quad \ldots(4.27)$$

$$F_{vn} = \frac{\mu_s F_x(h + t_b\mu_s) + (F_y + F_s + F_a)(x - h)}{(\cos\alpha + \mu_v\sin\alpha)(x - h - 2\mu_s R_v\sin\alpha) + \mu_s(\sin\alpha - \mu_v\cos\alpha)(t_b\mu_s + h + x - 2r_v(1 - \cos\alpha))} \quad \ldots(4.28)$$

$$F_{vt} = \mu_v F_{vn} \quad \ldots(4.29)$$

$$F_{t1} = \mu_s F_{n1} \quad \ldots(4.30)$$

$$F_{t2} = \mu_s F_{n2} \quad \ldots(4.31)$$

Where the last unknown ω_r may be obtained from eqn. (4.32) if a simplified analysis assuming steady roller rotation applicable.

$$\omega_r = \frac{(2\pi\eta\omega lR_e^2/\delta_2 - R_r F_{vt})\delta_2\delta_1}{2\pi\eta(lR_e^3\delta_1 + (R_r^4 - R_e^4)\delta_2)} \quad \ldots(4.32)$$

The value of ω_r for a more comprehensive study accounted for the angular acceleration (4,5,6) of the roller may be obtained by solving the dynamics equation of the rolling piston (see eqn. (4.33)) numerically.

$$I_r\dot{\omega}_r = M_{er} - R_r F_{vt} - M_{rc} \quad \ldots(4.33)$$

5. RESULTS AND DISCUSSIONS

The results presented here are predicted by applying geometrical dimensions of a machine designed for R12 operating at condensing temperature of 54.4°C and evaporating temperature at -23.3°C. The suction temperature of the machine was assumed at 32.2°C for all results predicted. The machine has a shaft input power of 123 *W* (when R12 is used) and the volume displacement of around 4.8 cc and it was designed to use R12 in refrigeration systems. It must be stressed that the model presented has yet to be verified with

the measured results. Only the results for the R12 have been very crudely compared with the available in house data. Experimental investigations are still under way. The results presented may only be stated qualitatively.

Since the existing system operates under $T_{evap} = -23.3°C$ and $T_{cond} = 54.4°C$ and the predictions presented here attempt to show how the system performance may be affected by CFCs alternative. To keep the T_{evap} and T_{cond} at the existing values, the operating pressures and the mass flowrate are altered. Table 1 shows the operating pressures for various freons under these postulated conditions. It shows that R134a has a highest compression ratio of 12.75 and followed by R12, R22 and R502. It also shows that the discharge pressures for R22 and R502 are significantly higher than R12 and R134a.

Figs. 4-7 show the predicted results for various freons, each operating under conditions tabulated in Table 1. Whereas Figs. 8-11 show the corresponding variations of instantaneous friction power loss for each frictional loss component. The friction loss between the eccentric face and the cylinder face is not presented as it is a constant value. Fig. 12 shows the corresponding total friction loss. It is assumed that the viscosities for the lubricant-refrigerant mixtures are the same in all cases. The variation in the friction power loss is thus caused by the difference in the chamber pressure variations.

The variation of pressure-angles for various refrigerants are shown in Fig. 4. It may be seen that the variation of pressures with angle corresponds to operating conditions given in Table 1. It shows that R22 and R502 operate at a higher pressure range as compared to R12 and R134a.

Refer to Table 2, as a result of these pressure variations the indicated power of R22 and R502 are 66% and 78% higher than that of R12. Whereas R134a is 7.8% lower than R12. These variations in indicated power are clearly illustrated in the pressure-volume diagrams shown in Fig. 5. Table 2 also indicates that a higher discharge pressure leads to a higher frictional power loss and vice versa. As a results R22, R502 show about 7% and 8% more friction loss compared to R12 and R134a is 1% higher.

Fig. 6 shows the variation in the chamber temperature. By assuming an adiabatic compression, the results show that the discharge temperature for R22 is significantly higher than the others whereas R134a has a lowest discharge temperature. In practice, these effects may affect the condensing temperature of the refrigeration system. The overall effects caused by these temperature differences will have to depend on the heat transfer between the refrigerant and the lubricating oil, especially during the discharge process. Where the latter process causes the two medium to be well mixed during the highly turbulent discharge flow condition.

A cooling capacity of a refrigerant system is dependent on the mass flowrate and the refrigerating effects. Fig. 7 shows that for different type of refrigerants, the mass induced is different. Table 2 tabulates the relative mass induced with respect to that of the R12. Due to the difference in suction pressures, R502 gives a higher mass flowrate than the rest and the lowest is R134a. At a higher suction pressure, a denser refrigerant vapour is induced and hence a higher mass flowrate resulted. The comparisons of the refrigerating effects at estimated evaporating conditions show that R22 has the highest refrigerating effects and followed by R12 and R502 whilst the minimum is R134a.

The cooling capacity is the product of the refrigerant mass flowrate and the refrigerating effects. From the comparisons it shows that the higher the mass flowrate the higher the cooling capacity:- R502 has a highest cooling capacity and the lowest is R134a. Comparisons of the EER shows that all refrigerants under these postulated operating conditions give very similar performance.

6. CONCLUSION

This preliminary studies assuming the same inlet temperature for all refrierants used, show that the compressor running on R12 will be penalised by about 6% loss in the cooling capacity if R134a is used. It also shows that if R22 and R502 are used as substitutes for R12, power input increases dramatically. Although the cooling capacity increases, but the overall gain in performance is marginal. It should be noted that these results are based on the assumptions in section 5.

The result also show that by maintaining the existing T_{evap} and T_{cond}, the power consumption, mass flowrate and the cooling capacity are affected. It shows that although R22 and R502 cause significant increase in the cooling capacity as compared to R12, however due to the increase in the power consumption, there appears no overall improvement (EER). For all the refrigerants tested, based on the assumptions mentioned, the results show insignificant variations in the values of EER.

When substituting existing CFCs to the new ozone friendly refrigerants, the thermodynamics performance of the machine should be considered as well as the availability of the suitable lubricant for the application, if the compatible materials are not readily available, the problem of using the new refrigerants will remain.

7. ACKNOWLEDGEMENT

The authors wish to thank Matsushita Refrigeration Industries (S) Pte Ltd for sponsoring this project. Special thanks to Mr Noriaki Okubo and Mr Khoo Chew Thong for their support and suggestions.

8. REFERENCES

1. Hamilton, J.F., Extension of mathematical modelling of positive displacement type compressors, short course text, Purdue University, 1974
2. Pandeya, P.N., Soedel, W., Rolling piston type rotary compressors with special attention to friction and leakage, Proceedings of the 1978 Purdue University Compressor Technology Conference
3. Ng, E.H., Tramschek, A.B., MacLaren, J.F.T., Computer simulation of a reciprocating compressor using a real gas equation of state, Proceedings of the 1980 Purdue University Compressor Technology Conference
4. Yanagiswa, T., Shimizu, T., Chu, I.,Ishijima, K. Motion Analysis of Rolling Piston In Rotary Compressor, Proceedings of the 1982 Purdue University Compressor Technology Conference
5. Yanagiswa, T., Shimizu, T., Friction losses in rolling piston type rotary compressors III, International Journal of Refrigeration, 1985.
6. Zhou, Z., Gong, Y., The estimation of the frictional losses of the rolling piston type refrigerant compressors, Proceedings of the 1988 International Compressor Engineering Conference At Purdue
7. Zhu, M., CFC Alternatives and their Thermophysical Properties in China, Far East Conference on Environmental Quality, Hong Kong, 1991
8. Downing, R.C., Fluorocarbon Refrigerants Handbook, Prentice Hall, 1988
9. Thermophysical Properties of Environmentally Acceptable Fluorocarbans HFC-134a HCFC-123, Japanese Association of Refrigeration and Japan Flon Gas Association, 1990
9. Statt, T.G., CFC Alternatives Recent Information concerning costs and efficiency, USNC/IIR Purdue Ref. Conference, 1990
10. Ramakrishan, K., CFC Issue: Social-Political Dimensions, Far East Conference on Environmental Quality, Hong Kong, 1991

	R12	R22	R502	R134a
Suction pressure (bar)	1.324	2.157	2.546	1.151
Discharge Pressure (bar)	13.46	21.47	23.076	14.68
Pressure ratio	10.17	9.95	9.06	12.75

Table 1 Operating pressures for various freons at $T_{evap} = -23.3°C$ and $T_{cond} = 54.4°C$

	R12	R22	R502	R134a
Normalised W_{ind}	1.000 (0%)	1.660 (+66%)	1.780 (+78%)	0.922 (-7.8%)
Normalised friction loss	1.000 (0%)	1.066 (+6.6%)	1.078 (+7.8%)	1.010 (1.0%)
Normalised shaft power	1.000 (0%)	1.577 (+57.5%)	1.682 (+68.2%)	0.934 (-6.6%)
Normalised $\dot{m}$	1.00 (0%)	1.17 (+17%)	1.80 (+80%)	0.72 (-28%)
Refrigerating effects, kJ/kg	143.97	193.26	137.03	186.40
Normalised estimated cooling capacity	1.00 (0%)	1.56 (+56%)	1.70 (+70%)	0.94 (-6%)
Normalised EER	1.00 (0%)	1.00 (0%)	1.01 (+1%)	1.00 (0%)

Table 2 Some performance parameters at $T_{evap} = -23.3°C$ and $T_{cond} = 54.4°C$ and $T_s = 32.2°C$.
Results are normalised relative to respective results for R12.

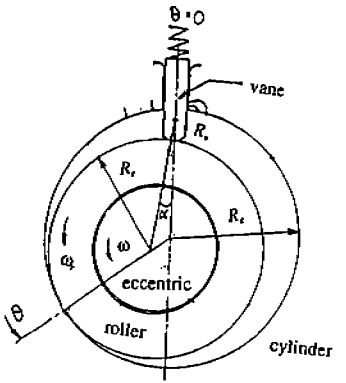

Fig. 1 Rolling piston compressor schematic

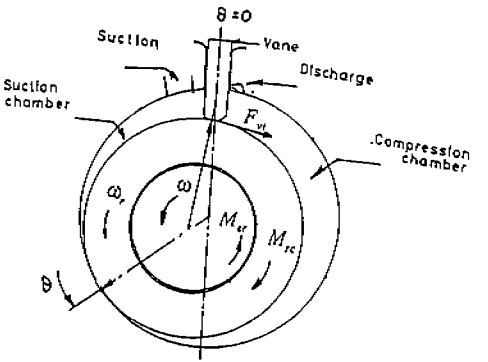

Fig. 2 Roller friction moments

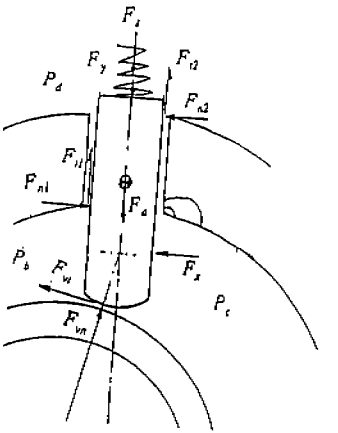

Fig. 3 Vane force balance

FIG. 4 PRESSURE–ANGLE HISTORY

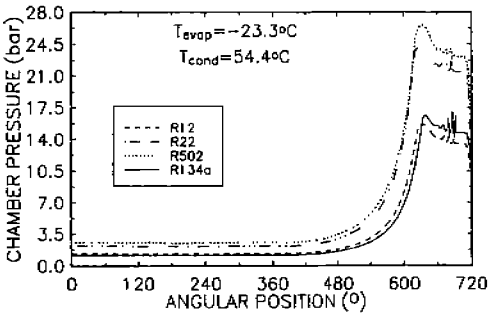

FIG. 5 PRESSURE–VOLUME HISTORY

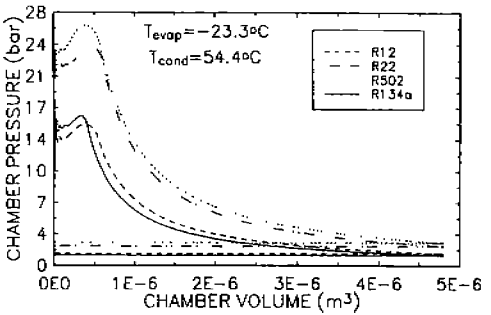

FIG. 6 TEMPERATURE–ANGLE HISTORY

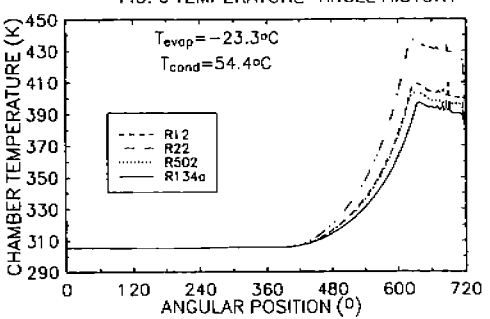

FIG. 7 CHAMBER MASS HISTORY

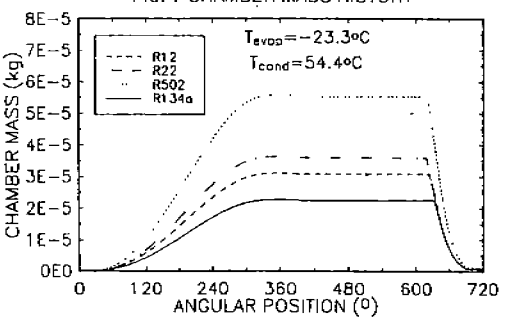

FIG. 8 VANE SIDE CONTACTS FRICTION LOSS

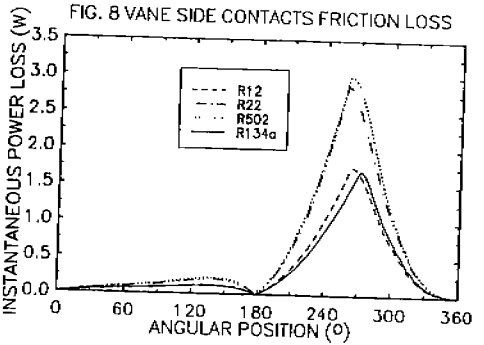

FIG. 9 VANE TIP CONTACT FRICTION LOSS

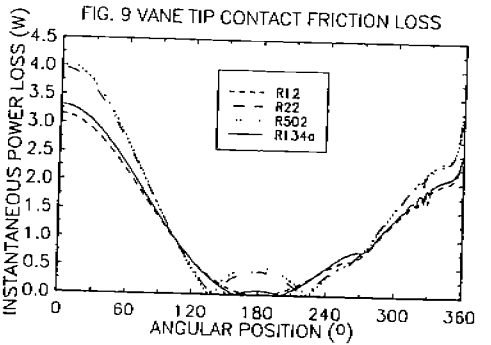

FIG. 10 ROLLER–ECCENTRIC FRICTION LOSS

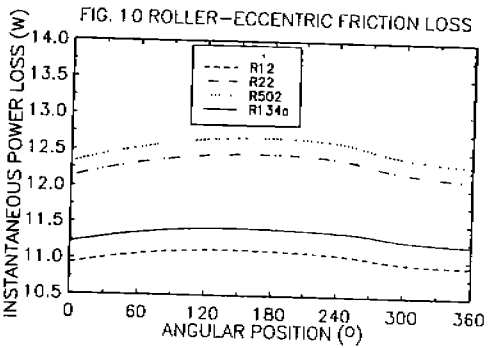

FIG.11 ROLLER–CYLINDER HEAD FACE FRICT. LOSS

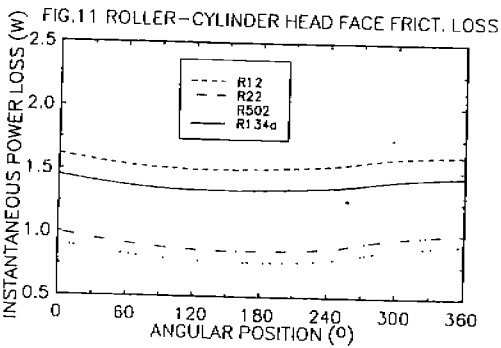

FIG.1 2 TOTAL FRICTION LOSS